Correcting the Energy Reconstruction of Photons Detected in the Electromagnetic Calorimeter

Johnathon K. Upperman
Office of Science, Science Undergraduate Laboratory Internship Program
Correspondence: jo1232hn@yahoo.com

The College of William and Mary, Williamsburg

Thomas Jefferson National Accelerator Facility
Newport News, Virginia

July 30, 2009

Prepared in partial fulfillment of the requirement of the Office of Science, Department of Energy's Science Undergraduate Laboratory Internship under the direction of Francois-.X Girod at the Thomas Jefferson National Accelerator Facility.

ABSTRACT

Correcting the Energy Reconstruction of Photons Detected in the Electromagnetic Calorimeter.
JOHNATHON K. UPPERMAN (The College of William and Mary, Williamsburg, VA 23187)
FRANCOIS X. GIROD (Thomas Jefferson National Accelerator Facility, Newport News, VA 23606).

The outermost layer of the Continuous Electron Beam Accelerator Facility (CEBAF) Large Acceptance Spectrometer (CLAS) at the Thomas Jefferson National Accelerator Facility consists of an electromagnetic calorimeter (EC). The EC is composed of alternating layers of scintillator strips and lead sheets and covers a large portion of the angular range. The EC is used to detect particles—such as electrons, photons, and neutrons—that meet a certain energy threshold. When a particle enters the EC, it loses some of its energy and creates a shower of light that is picked up by the scintillators. The location and amount of this detected light is then used to help identify where and with what energy a particle entered the EC. However, this system has some inefficiency built into it; for example, its layers of lead absorb some of the light instead of recording it. Since the EC contains some unavoidable inefficiency and particles do not always deposit all of their energy, the energy recorded in the EC needs to be analyzed periodically to determine what corrections need to be made to identify the true energy of incident photons. Creating the correction helps to better identify photons and to better understand the intrinsic inefficiency in the EC. The focus of this project was to create a correction for the energy of photons detected in the EC and then use this correction to understand EC inefficiency. To do this, a reaction was picked that involves only electrons, protons, and neutral pi mesons that decay into two photons. The invariant mass of the photon pairs, which were considered to have originated from the same decay, was then compared to the known theoretical mass of the neutral pi meson. The known mass was used to identify how the energy of photons needed to be corrected for different energy levels. It was found that a correction function could be created to

increase the accuracy of photon reconstruction. The correction function that was discovered varies considerably from a previous correction that was implemented in 2006. The new correction will be used to analyze data that contain photons at 0.3 GeV and greater. With this new correction implemented, the efficiency of assigning energy to incident photons in the EC has increased. Also, we used this information to estimate the overall efficiency of the EC in detecting photons—a process that hasn't been performed previously on CLAS.

INTRODUCTION

Creating a three-dimensional picture of the proton is one important project currently underway at the Thomas Jefferson National Accelerator Facility (Jefferson Lab). The picture of the nucleon is being formed by probing its inner composition (i.e. its quarks and gluons). As the project progresses, different properties of the proton such as its mass, spin, and magnetic moment are hoped to be understood more thoroughly [1].

One method of performing proton tomography makes use of the process called Deeply Virtual Compton Scattering (DVCS). DVCS occurs when the accelerated electron beam hits a hydrogen target and scatters (emitting a virtual photon that is absorbed by the quark) not from the entire proton, but from one of the quarks within the proton [2]. After the quark absorbs the virtual photon, it releases a real photon, with the same energy, that is measurable.

Since the energy of the real photon corresponds to the energy of the virtual photon, it is important to accurately measure the energy of photons emitted during DVCS. The CEBAF Large Acceptance Spectrometer (CLAS), in hall B, measures the energy of incident photons with its electromagnetic calorimeter (EC). The calorimeter is composed of alternating layers of

scintillator strips and lead sheets. When a particle enters the EC, it creates a showering of light that is collected by the scintillators then sent to photomultiplier tubes (PMTs) for readout [3].

However, the scintillator has about a 1/3 effective thickness whereas the lead has a 2/3 effective thickness; therefore, much of the light emitted is absorbed by the lead and not recorded [4]. This problem creates a built-in inefficiency in the EC that needs to be periodically studied so that it can be taken into account.

The aim of this experiment was to create a correction for photons detected in the EC and then use the correction to study the error in the EC. Correcting the energy of photons and understanding the efficiency of the EC will increase the accuracy of particle identification in CLAS.

METHODS

i . Plan

A program was written to analyze the E01-113 set of data collected in 2005 in the hall B CLAS detector system. The following series of reactions were studied:

Electron beam + Proton target -> electrons + protons + neutral pi mesons (1)

Neutral Pi meson -> 2 Photons (2)

First, conditions were specified to ensure proper identification of electrons, protons, and photon pairs. Then, conditions were set to find (1) reactions. The theoretical mass of the neutral pi meson, 135 MeV/c^2 , was used as a constraint for the energies of the photon pairs.

Once the correction was determined, it was used as part of the process in estimating the overall efficiency of the EC.

ii. Good Trigger Electron Identification

The first particle was required to have one negative elementary charge. A cut was implemented that excluded particles that deposited energy below 0.06 GeV in the inner layer of the EC. A cut was implemented that constrained the particle to have come from within 5 cm of -66.5 cm z (the location of the target). For a histogram of this variable, see figure 1. For a graph of the geometrical location of electron hits in the EC, see figure 2.

To distinguish between electrons and negative pi mesons at low momentum, a minimum signal, > 2.5 photoelectrons, was required in the Cherenkov counter (CC); for a histogram of the number of photoelectrons see figure 3. This cut is more than 99% efficient until particles reach a momentum of 2.5 GeV/c, then at higher momentum a cut is implemented in the EC that is efficient from 1.5 GeV/c to higher momentum [7]. The cut for the energy detected in the EC depended on the sector that the particle was detected in because the sampling fraction (energy deposited divided by momentum) as a function of momentum varied for each sector—see figure 4. For each sector the following cut was implemented:

$$\frac{Energy\ deposited}{p} - \mu(p) < 3.5 * \sigma(p) \qquad (3)$$

Where $\mu(p)$ and $\sigma(p)$ are the mean value and sigma, respectively, that depend upon the momentum.

iii. Proton Identification

The next particle was required to have one positive elementary charge. A cut was implemented that required the particle to have a momentum greater than 0.2 GeV/c so as to clear up poor resolution effects. A cut on where the next particle left the z axis was implemented. The cut went as follows:

$$|Proton\ Z\ position - Electron\ Z\ position| < 3.5 \times \left(0.75 + \frac{0.134}{Proton\ momentum^2}\right) \quad (4)$$

This cut depends on the momentum of the proton because at lower momentum the proton makes a path with a larger curvature in the detector and it becomes more difficult to determine where the path originated—see figure 5 [4].

The beta of the proton can be determined in two ways. The first way to determine the beta of the proton is to use the path length, and time of flight as detected by CLAS—see (5). The second method is to calculate the beta using the momentum detected and the theoretical mass of the proton—see (6).

$$\frac{R}{c \times t} \quad (5)$$

$$\frac{p}{\sqrt{p^2 + m^2}} \quad (6)$$

The time (t), in (5), includes the trigger time correction. The difference of the beta calculated from (5) and (6) was required to be below 0.05. To see (5) plotted as a function of the proton's momentum, see figure 6. For more information about this technique see [5].

iv. Photon Identification

The next particle was required to have an elementary charge of zero. A cut was implemented that required the momentum to be greater than 0.1 GeV/c. Since a photon's beta is one, particles that were reconstructed with a beta less than 0.92 were cut. For a histogram of the beta of the detected photons, see figure 7. For a plot of geometrical location of photon hits in the EC, see figure 8.

v. Using e(-) + p(+) -> e(-) + p(+) + x reactions to identify neutral pi mesons

The invariant mass of potential photon pairs was reconstructed using the following relationship.

$$IM(\gamma_1\gamma_2) = \sqrt{2 \times E1 \times E2 \times \left(1 - cos\theta_{\gamma_1\gamma_2}\right)} \quad (7)$$

E1 and E2 are the respective energies of the photon pairs as detected in the EC—photon one was defined as the photon with larger energy. $\theta_{\gamma_1\gamma_2}$ is the angle between the two photons after they decayed from the neutral pi meson. $\theta_{\gamma_1\gamma_2}$ was determined using the locations of the photon pairs as they were detected in the EC. A cut was implemented that required the opening angle to be greater than 3.5˚ which can be seen in figure 9. The minimum angle is determined by (8) and constrained by (9).

$$\theta_{\gamma_1\gamma_2}^{min} = 2 \times \tan^{-1}\frac{m_{\pi^0}}{E_{\pi^0}} \quad (8)$$

$$E_{\pi^0} = E_{beam} + M_{target} - E_{e^-} - E_{p^+} \quad (9)$$

Using conservation of energy and momentum, the missing mass squared (MM^2) of the neutral pi meson was plotted. The MM^2 was calculated using equations (10) – (12).

$$E_{\pi^0} = 5.776 + 0.938 - E_{e^-} - E_{p^+} \quad (10)$$

$$P_{\pi^0} = P_{beam} - P_{e^-} - P_{p^+} \quad (11)$$

$$MM^2 = E^2_{\pi^0} - P^2_{\pi^0} \quad (12)$$

5.776 GeV is the energy of the beam. 0.938 GeV/c^2 is the mass of the proton. The calculated neutral pi meson MM^2 can be seen in figure 10.

The MM^2 of the proton was calculated by rearranging (10) – (12). The energy and momentum of the neutral pi meson were determined using the detected photons. In the last plot of the proton MM^2, the photon energies used included the correction function. The calculated proton MM^2 can be seen in figure 11.

Before the correction function was determined the following constraints were enforced to ensure exclusive neutral pi meson events. The missing momentum in the x and y direction were required to be small so as to ensure that all momentum had been accounted for. The proton angle was fitted by equation (13) which can be seen in figure 12. The neutral pi meson angle was cut by equation (14)—see figure 13. Also, the MM^2 of the neutral pi meson and the proton were cut on—see figure 14.

$$\theta_{p^+} < \frac{50}{\left([P]_{p^+} + 0.5\right)^2} \quad (13)$$

$$\theta_{\pi^0} < \frac{28}{\left([E]_{\pi^0} + 1\right)^2} \quad (14)$$

θ_{p^+} and θ_{π^0} symbolize the angles between the predicted direction of the particle and the measured direction of the particle for the proton and neutral pi meson respectively. The

predicted direction, for both particles, was found using conservation of momentum and energy principles.

vi. Calculating the correction function for photons

The method used in [6] was used to make the correction for photon energies. The theoretical mass of the neutral pi meson (0.135GeV/c^2) can be written as:

$$m_{\pi^0} = \sqrt{\frac{E_{\gamma_1}}{corr(E_{\gamma_1})}} \times \sqrt{\frac{E_{\gamma_2}}{corr(E_{\gamma_2})}} \times 2\sin\theta_{\gamma_1\gamma_2} \qquad (15)$$

In (15) E_{γ_1} and E_{γ_2} stand for the measured energies of the photons and corr($E_1(\gamma_1 1)$) stands for the sought out correction that depends upon the measured photon energy. Then, the ratio of (7) and (15) can be written as:

$$\frac{IM(\gamma_1\gamma_2)}{m_{\pi^0}} = \sqrt{corr(E_{\gamma_1}) \times corr(E_{\gamma_2})} \qquad (16)$$

For the first step of the correction, both photons were required to be within the same energy range. When both photons have nearly equal energy (16) becomes:

$$\frac{IM(\gamma_1\gamma_2)}{m_{\pi^0}} = corr(E_{\gamma_1}) \qquad (17)$$

With this in mind, ten histograms were made of the $IM(\gamma_1\gamma_2)$ for ten different energy ranges—see figure 15. The first histogram required the two photons to be between 0.255 GeV and 0.315 GeV; then, the allowed energy increased in 70 MeV steps. The histograms in figure 15 were fitted with a Gaussian plus a linear background and the Gaussian mean divided by m_{π^0} was plotted as a function of E_{γ_1}. The graph was then fitted with a function:

$$corr(E) = a + \frac{b}{E} + \frac{c}{E^2} \qquad (18)$$

The contribution step one made to (18) can be seen by the red line in figure 15 and figure 16. In comparison, the blue line in figure 15 is the result from [6]. The result from [6] is also in figure 16—it is the line that begins to flatten out near one.

For the second step, if one of the photons was in the correction range (0.3 – 1.135 GeV), then that photon was corrected using (17). The correction for the other photon could then be calculated using (16). For example, if the energy of the first photon (defined as the most energetic) was within the range where (17) was valid, then that photon was corrected using (17). Rearranging (16) the correction for the second photon becomes:

$$corr(E_{\gamma_2}) = \frac{IM(\gamma_1\gamma_2)^2}{m_{\pi^0}^2} \qquad (19)$$

In (19) $IM(\gamma_1\gamma_2)$ includes the correction for the energy of the first photon. When the most energetic photon was within where (17) is valid, the second correction was used to fill the portion below 0.3 GeV. When the least energetic was within where (17) is valid, the correction for the most energetic was used to fill the portion above 1.135 GeV. As in the first step, the mean value of the $IM(\gamma_1\gamma_2)$ for the different energy bins was divided by 0.135 GeV and plotted as a function of the energy of the most energetic photon. To see the $IM(\gamma_1\gamma_2)$ from step two see figure 16. The correction, including the second step, can be seen in figure 16 as the black line.

vii. Estimating the detection efficiency of the EC

To estimate the detection efficiency, two data trees were created. In one tree, both photons from the neutral pi meson decay were detected in the EC. While in the other tree, one

photon was detected and the missing energy of the second photon was calculated. Both trees used the correction function for the energy of the photons detected.

Before the trees were compared a series of cuts were implemented on both. The opening angle between the two photons was constrained from above and below using (20). Also, the energy of the most energetic photon was required to be greater than 0.5 GeV. The mass squared of the neutral pi meson was constrained by (21). If in the data a mass was associated with the second photon, the mass was kept to a minimum using (22).

$$\left[2 \times \tan^{-1}(\square)\left[\frac{0.09}{E_{\gamma_1}+E_{\gamma_2}}\right)\right] < \theta_{\gamma_1\gamma_2} < \left[2 \times \tan^{-1}(\square)\left[\frac{0.25}{E_{\gamma_1}+E_{\gamma_2}}\right)\right]$$

(20)

$$m_{\pi^0}^2 < \left[0.3 - \left(0.08 \times E_{\gamma_1}\right)\right] \quad (21)$$

$$m_{\gamma_2}^2 < \left[0.117 - 0.035 \times E_{\gamma_1}\right] \quad (22)$$

After the above cuts were made, the phi vs. theta of the second photon was plotted in figure 17. In figure 17, it was believed that the same sample of events were obtained. Then, a geometrical cut was implemented on figure 17 for both data trees. The geometrical cut on the second photon required theta to be greater than 19.5° and less than 35°; also, the cut restricted each segment of phi to 15°. The middle of the segments was determined by using the left graph in figure 17, which shows the actual geometrical acceptance of the EC. Once the geometrical cut was enforced, the number of events in both trees were compared in figure 18.

RESULTS

i. The correction function for photons

The correction function for photons was found to be:

$$corr(E) = 1.07 - \frac{0.1065}{E} + \frac{(0.0105)}{E^2} \quad (23)$$

The correction function can be seen in figure 16. Using (23), the $IM(\gamma_1\gamma_2)$ can be written as:

$$IM(\gamma_1\gamma_2) = \sqrt{\frac{E_1}{corr(E_1)}} \times \sqrt{\frac{E_2}{corr(E_2)}} \times 2\sin\frac{\theta_{\gamma_1\gamma_2}}{2} \quad (24)$$

The $IM(\gamma_1\gamma_2)$ given by (24) can be seen in figure 19.

ii. Estimate of the detection efficiency of the EC

By comparing the integrals of each graph in figure 18, it was estimated that the EC is about 95% efficient in detecting photons.

DISCUSSION and CONCLUSION

i. The correction function for photons

A new correction function for photons in EC was found for e1dvcs. The correction function is valid for photons from 0.2 – 3.2 GeV and will be used in future analysis of this data. The efficacy of the correction can be seen in figure 19. Figure 19 shows that the mean value of the $IM(\gamma_1\gamma_2)$, using the correction function, is 0.1342 GeV. The method used to determine the correction function is unique because the proton was also identified; whereas, the proton was not identified in [6]. For a thorough discussion of systematic errors involved in this process see [6].

ii. Estimating the detection efficiency of the EC

The e1dvcs aims at publishing both DVCS and neutral pi meson electroproduction cross-sections soon. The result of this study is important to have because the estimate is needed when conducting experiments measuring cross-section. The EC efficiency has been estimated in other experiments using electrons. For theoretical reasons, photons and electrons are expected to be detected with a similar efficiency in the EC. Previously, only the detection efficiency for electrons has been determined because it is easier to estimate the electron efficiency since it is detected by every part of CLAS. All previous estimates of the EC efficiency using electrons give the same value: 95 +/- 1% [8]. Thus, this study supports the theoretical assumption.

The estimated efficiency of the EC determined in this paper must be further studied by performing checks with simulations including radiatiative effects.

FIGURES

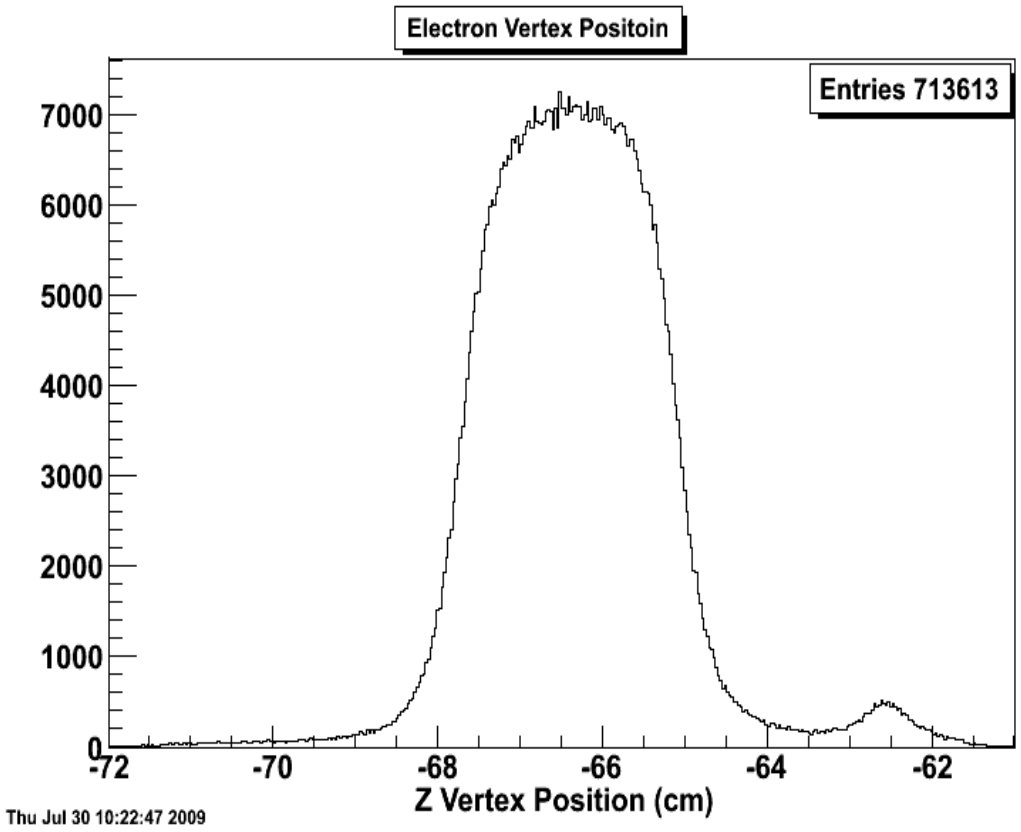

Figure 1

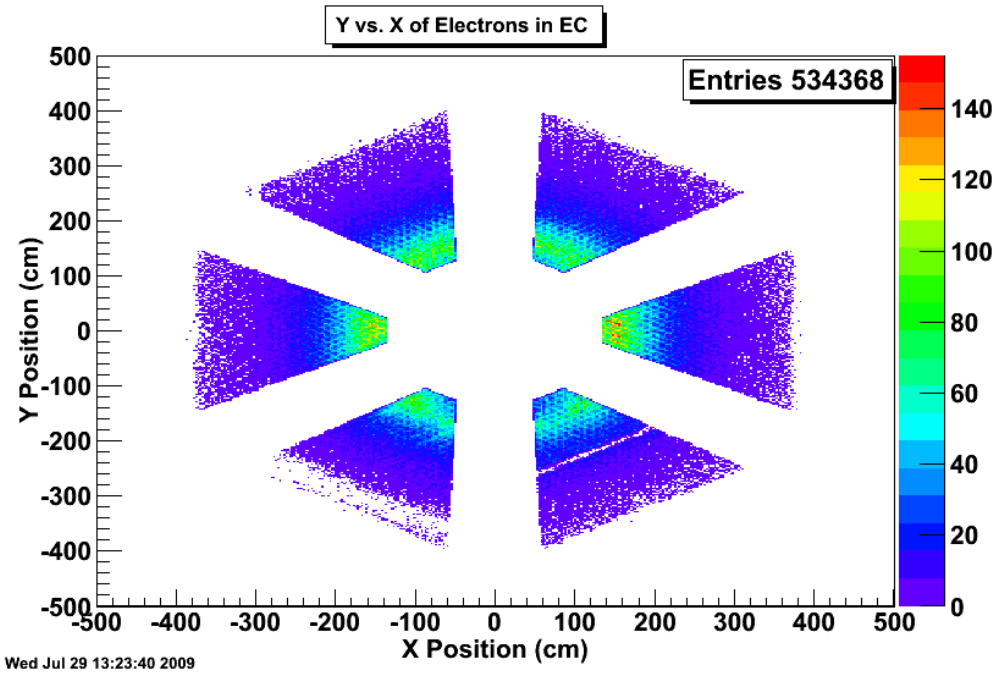

Figure 2

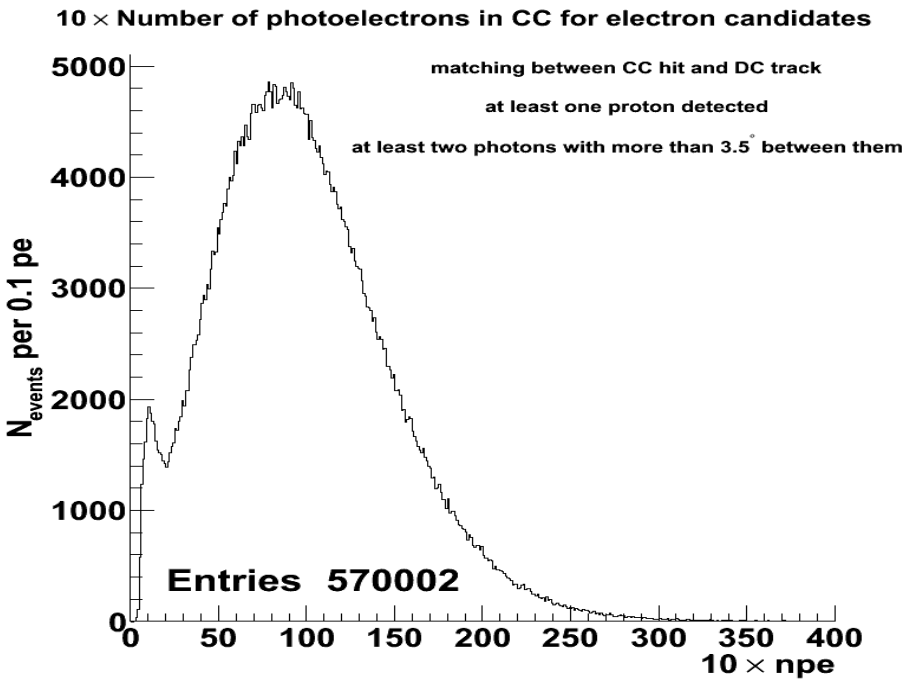

Figure 3

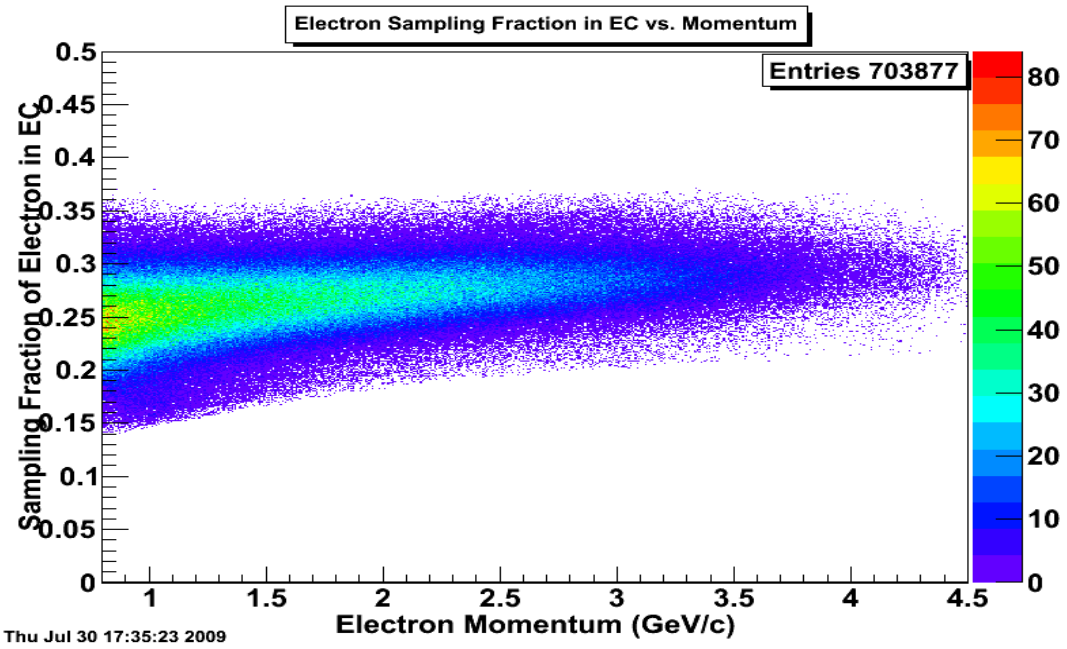

Figure 4: electron sampling fraction for all sectors. The sampling fraction is equal to the energy deposited in the EC divided by the total momentum of the electron. Figure 4 shows that the electron roughly deposits a third of its energy in the EC.

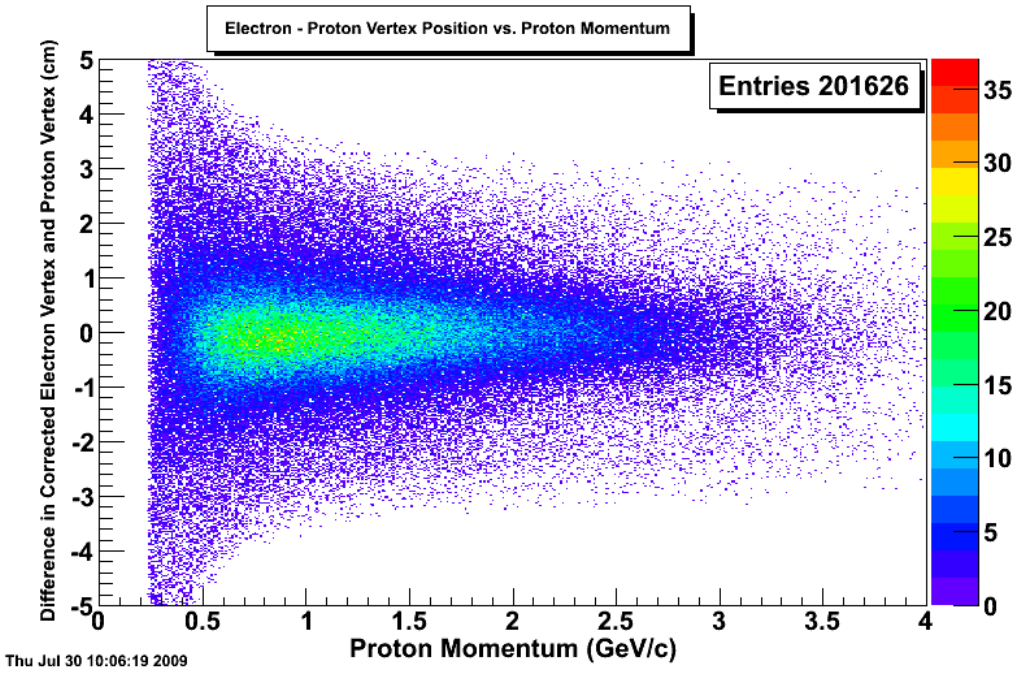

Figure 5

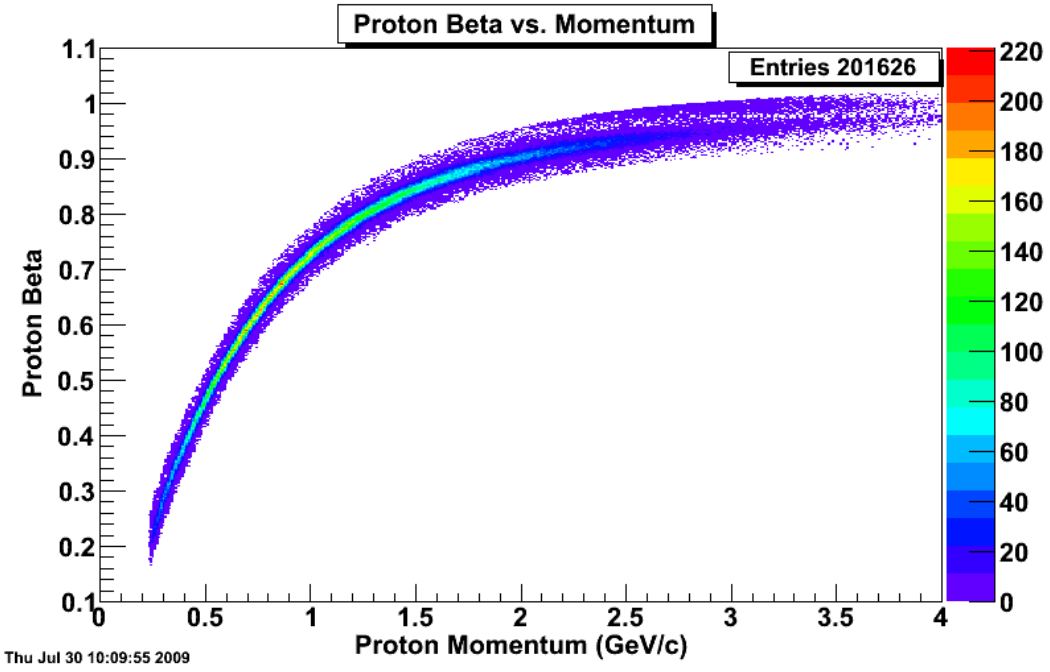

Figure 6: Proton beta (as measured in TOF scintillators) after cut versus momentum.

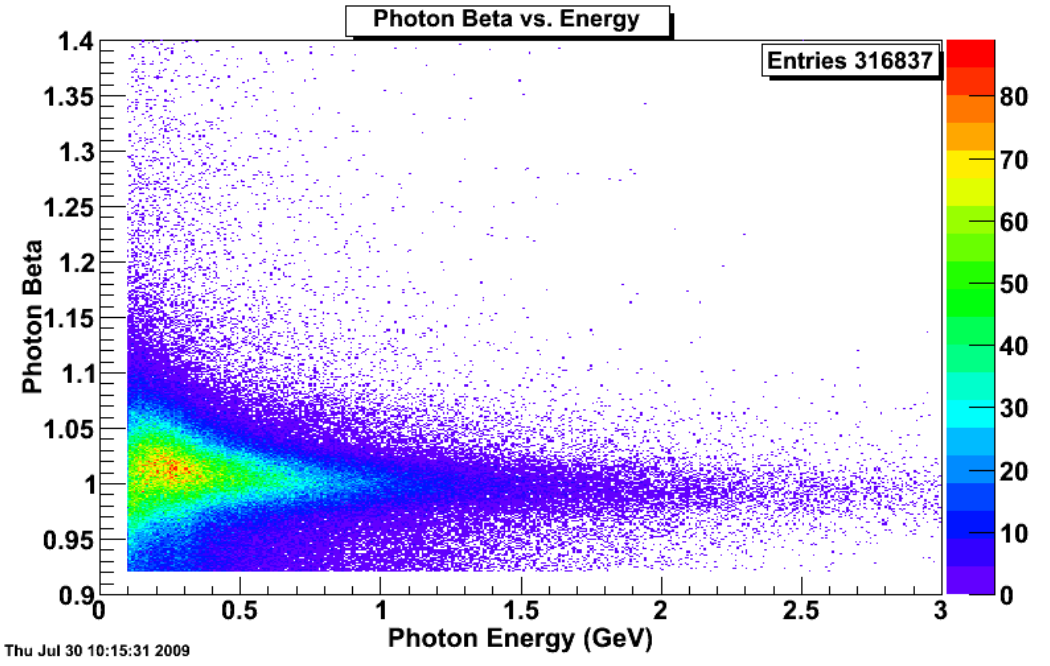

Figure 7: Photon beta measured in EC versus photon energy.

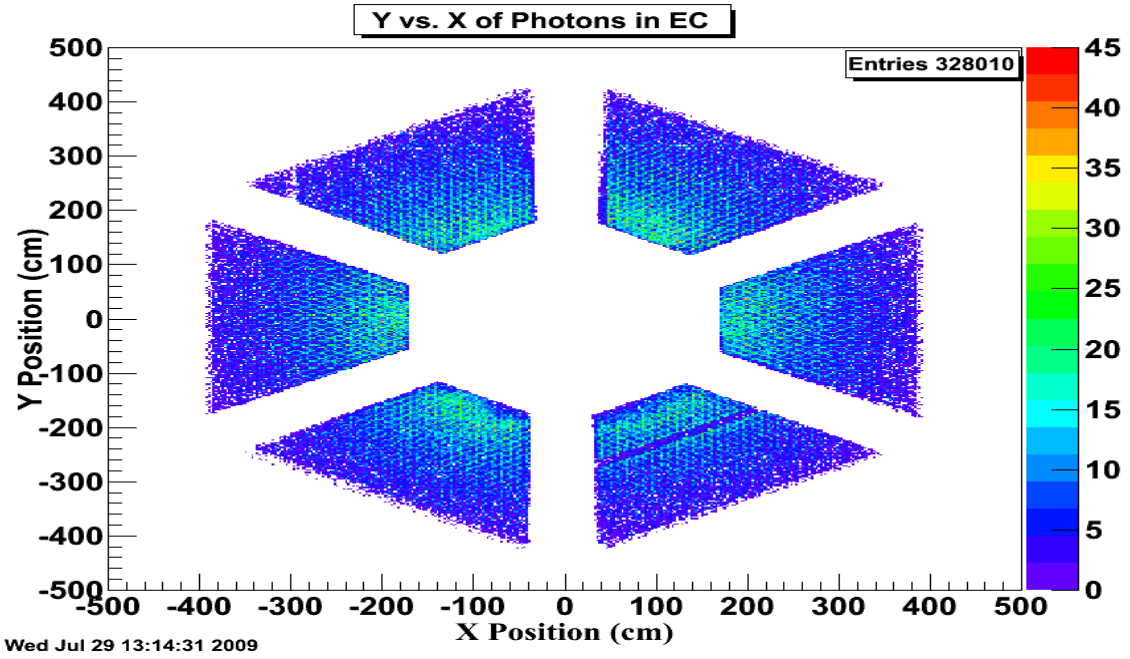

Figure 8

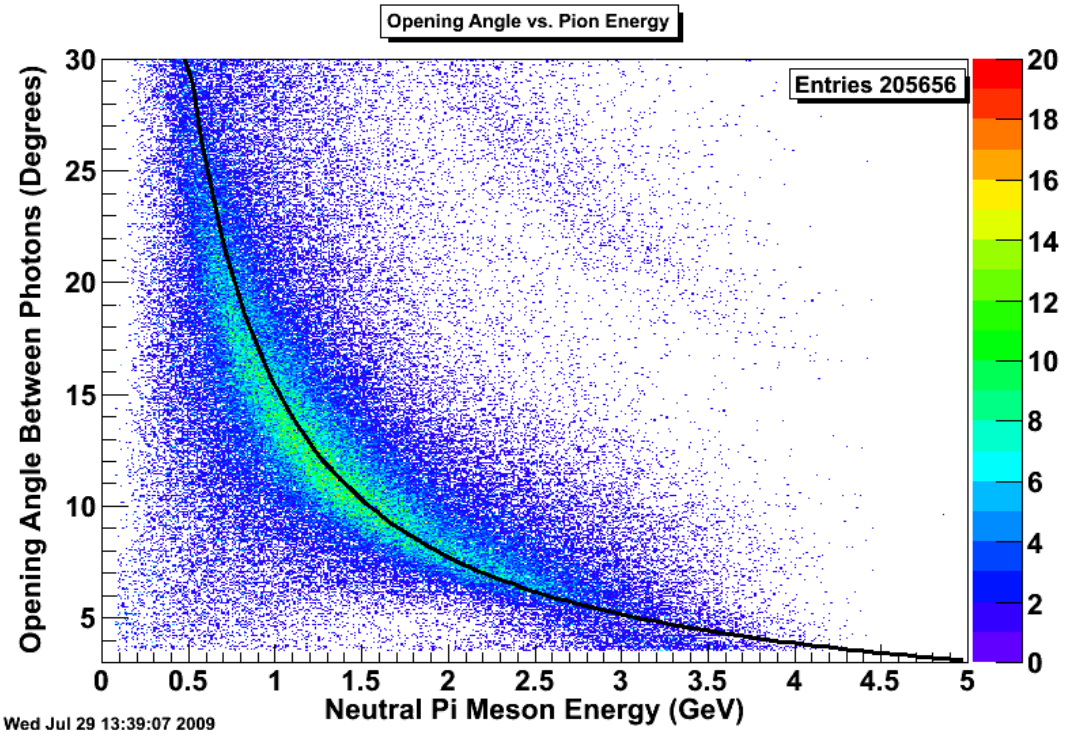

Figure 9: Opening angle between the two photons in neutral pi meson decay versus neutral pi meson energy. The black curve corresponds to the theoretical curve.

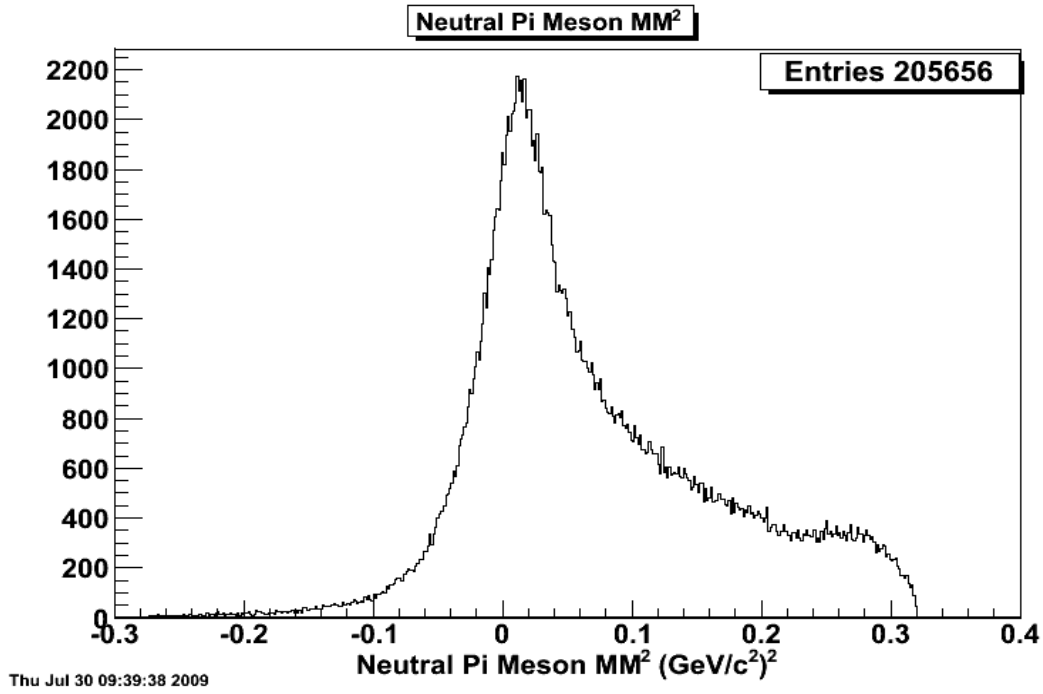

Figure 10: Missing mass squared of the electron and proton system for exclusive electron, proton, and neutral pi meson producing events.

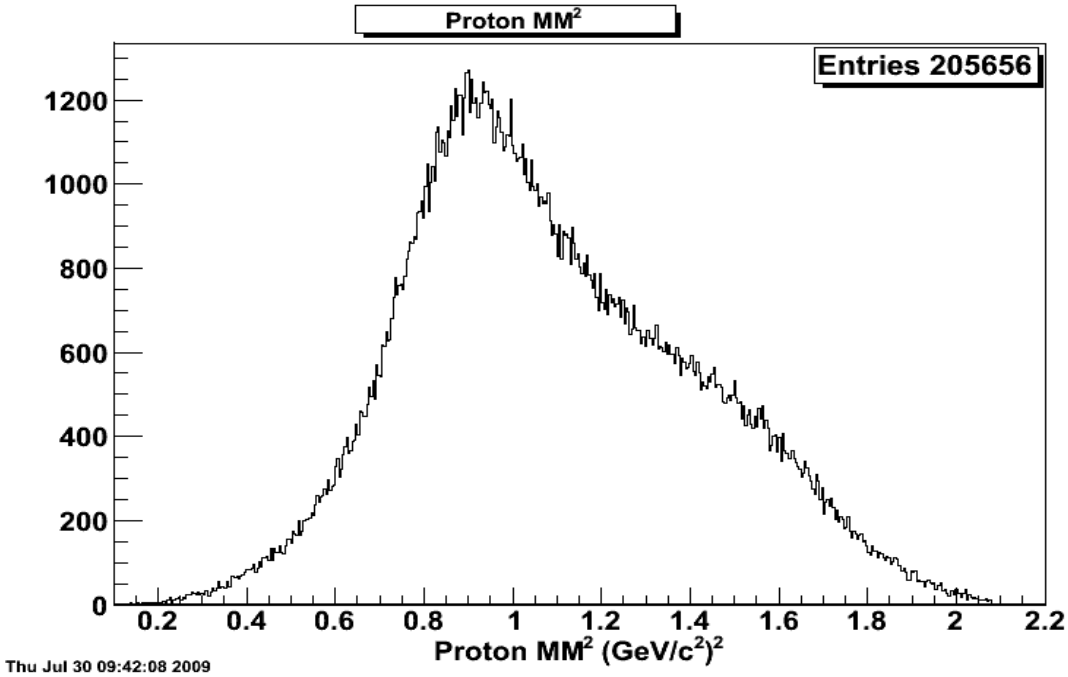

Figure 11: Missing mass squared of the electron and neutral pi meson system for exclusive electron, proton, and neutral pi meson producing events.

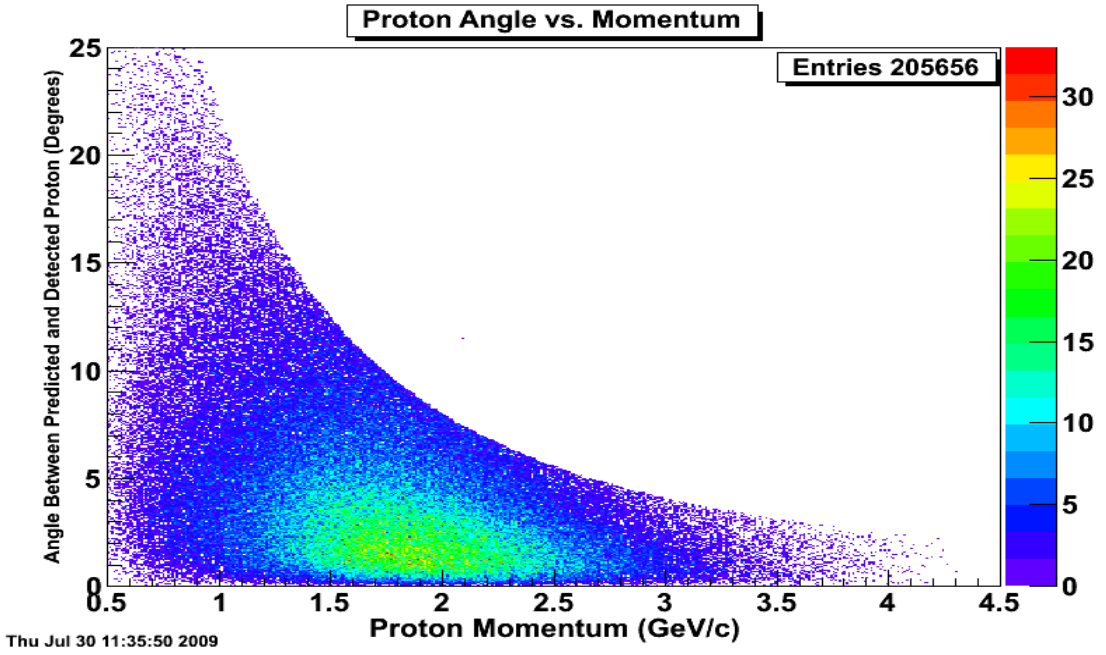

Figure 12

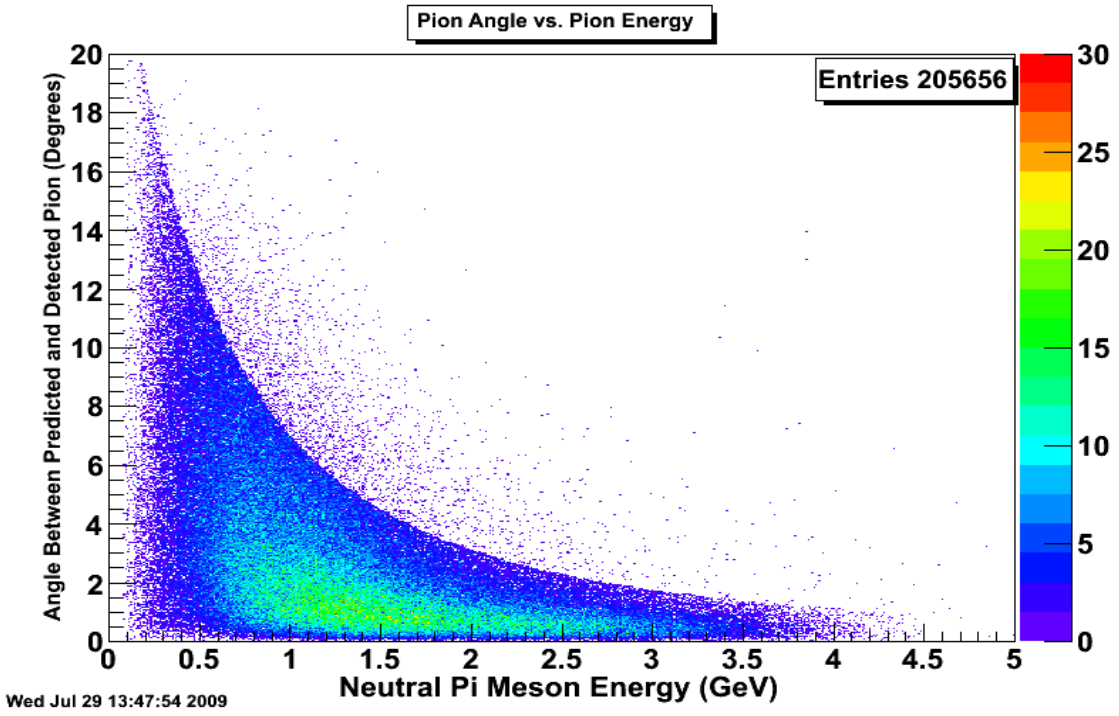

Figure 13

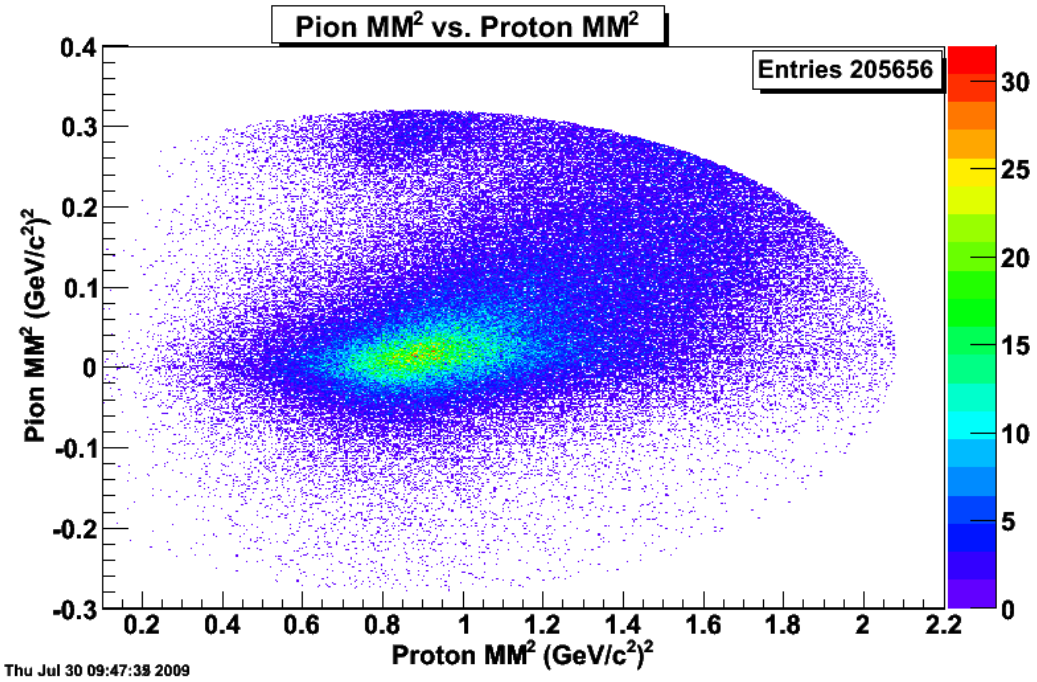
Pion MM² vs. Proton MM²
Entries 205656
Pion MM² (GeV/c²)²
Proton MM² (GeV/c²)²
0.4
0.3
0.2
0.1
0
-0.1
-0.2
-0.3
0.2
0.4
0.6
0.8
1
1.2
1.4
1.6
1.8
2
2.2
30
25
20
15
10
5
0
Thu Jul 30 09:47:38 2009

Figure 14

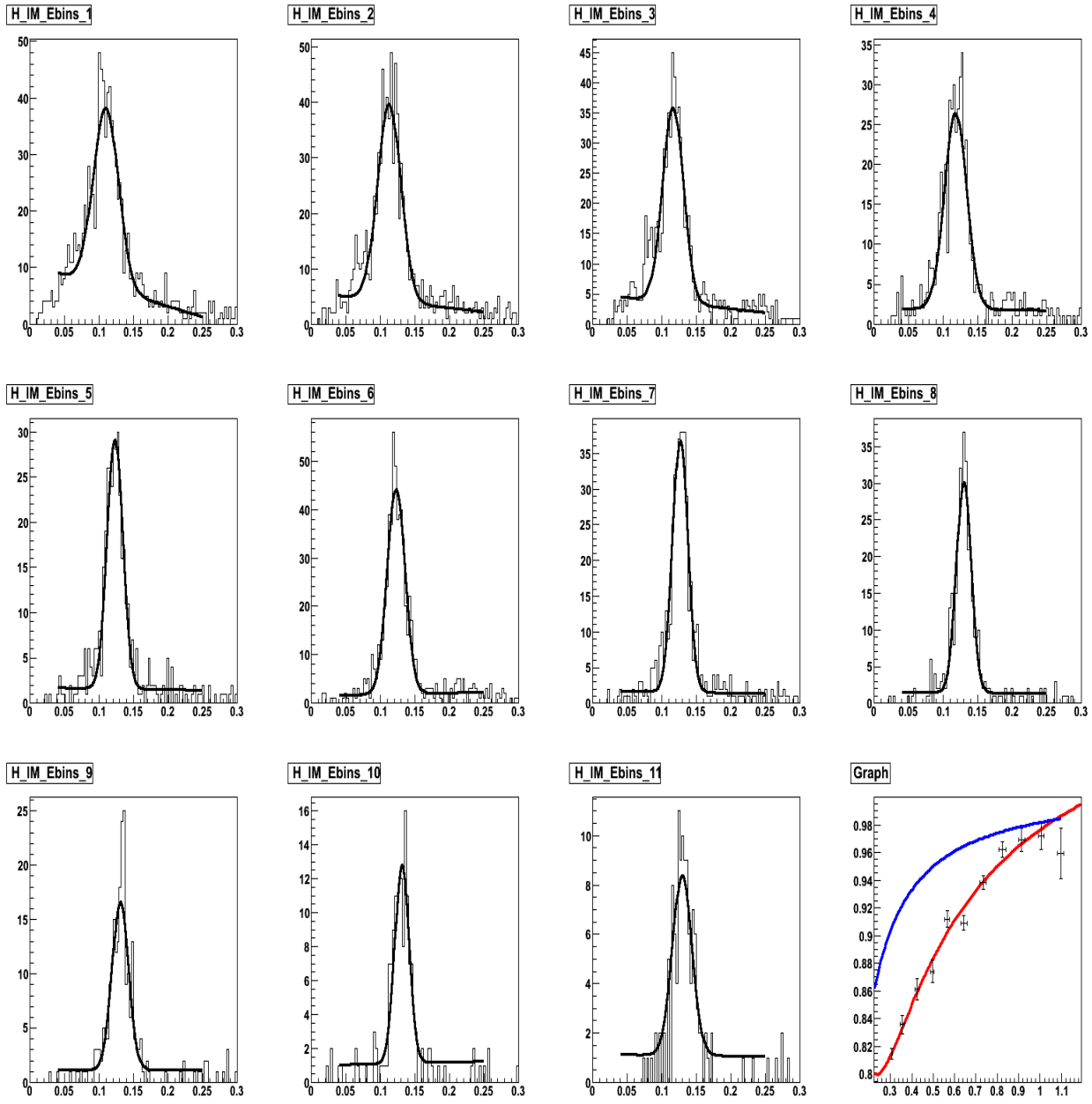

Figure 15: From left to right and to bottom: Invariant mass of the photon pairs for progressing energy bins fitted with a Gaussian plus a linear background. The bottom right: mean value of the Gaussian as a function of the mean energy in the bin. The red curve is the fit to data points. The blue curve is the result previously found in 2006.

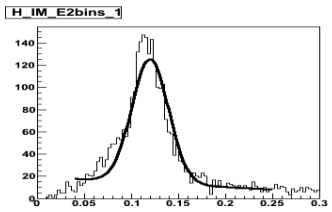
H_IM_E2bins_1

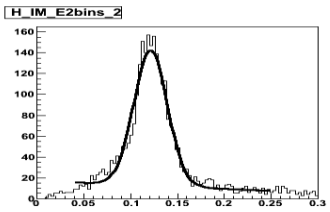
H_IM_E2bins_2

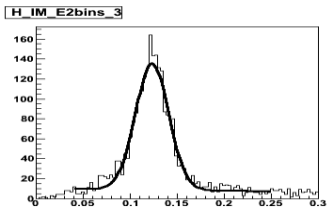
H_IM_E2bins_3

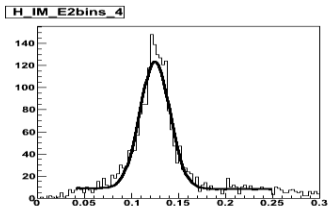
H_IM_E2bins_4

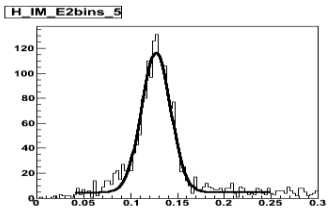
H_IM_E2bins_5

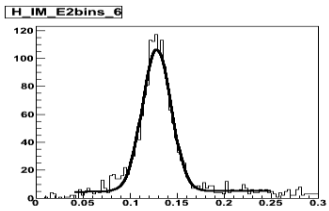
H_IM_E2bins_6

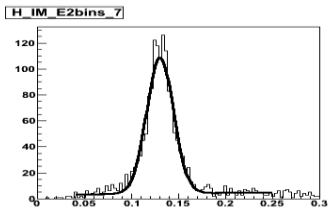
H_IM_E2bins_7

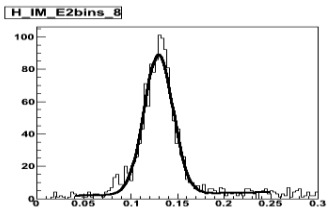
H_IM_E2bins_8

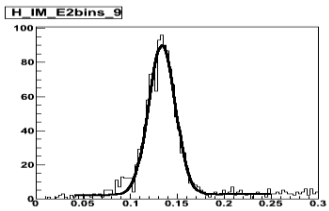
H_IM_E2bins_9

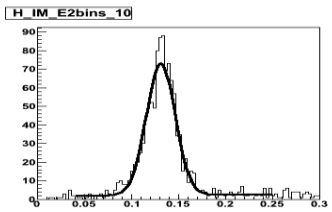
H_IM_E2bins_10

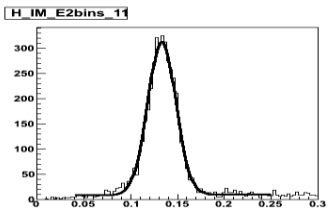
H_IM_E2bins_11

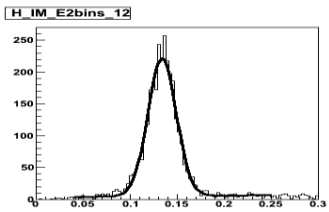
H_IM_E2bins_12

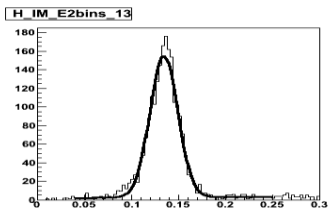
H_IM_E2bins_13

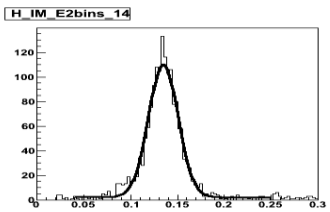
H_IM_E2bins_14

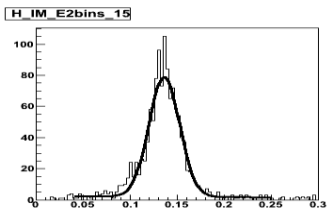
H_IM_E2bins_15

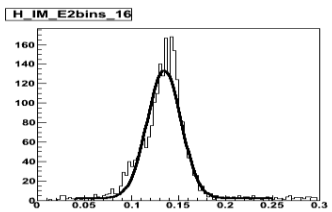
H_IM_E2bins_16

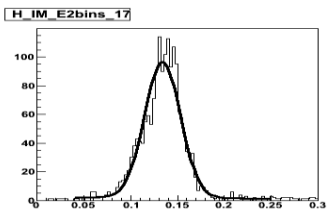
H_IM_E2bins_17

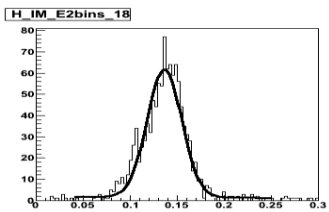
H_IM_E2bins_18

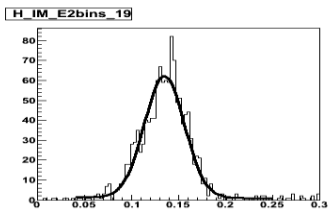
H_IM_E2bins_19

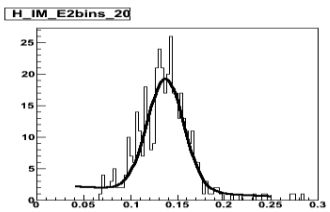
H_IM_E2bins_20

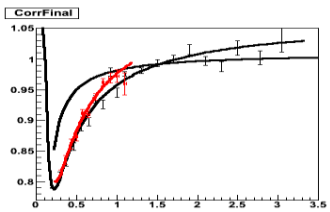
CorrFinal

Figure 16: Same as in figure 15, but for the second step. The curve that flattens near one corresponds to the results found previously in 2006.

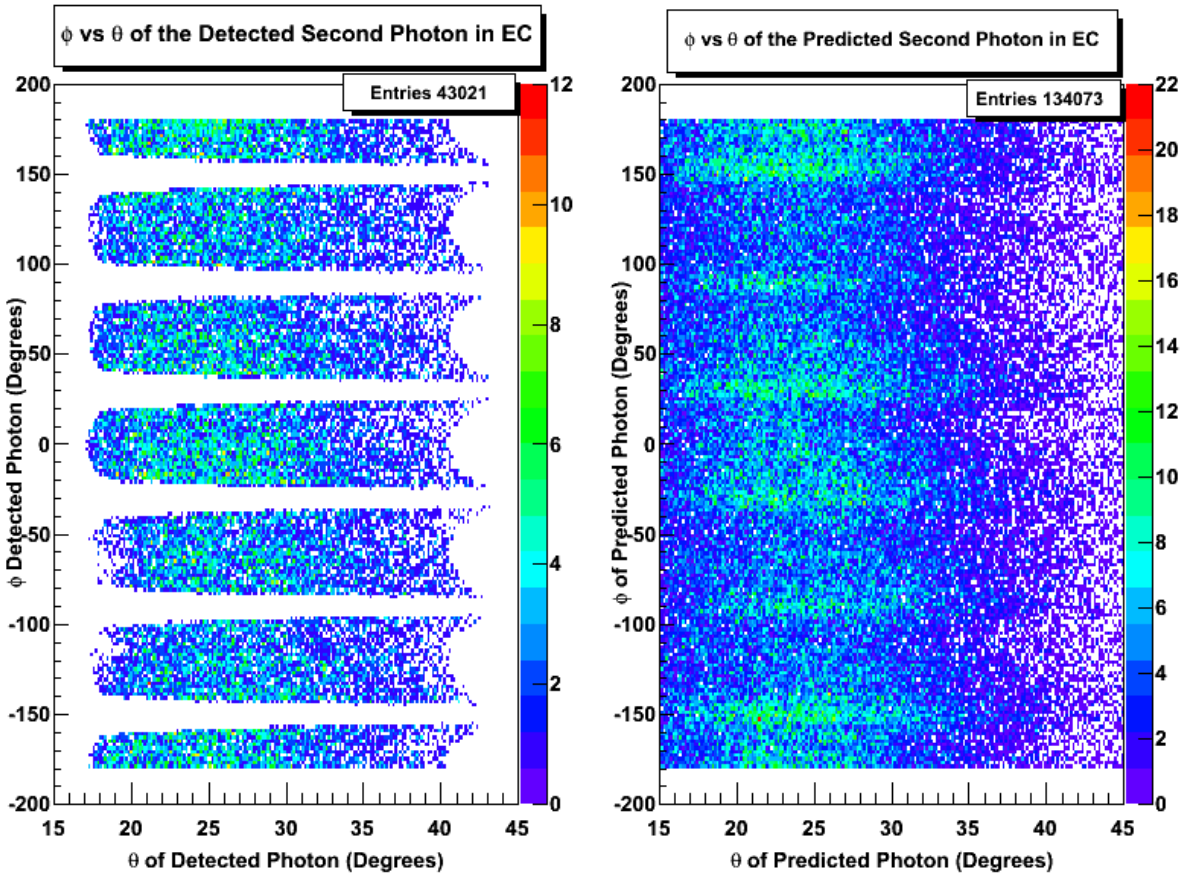

Figure 17: The plot on the left shows events that were detected and is thus limited to the location of the EC. The plot on the right shows the predicted location of photons and therefore is not restricted by the location of the EC.

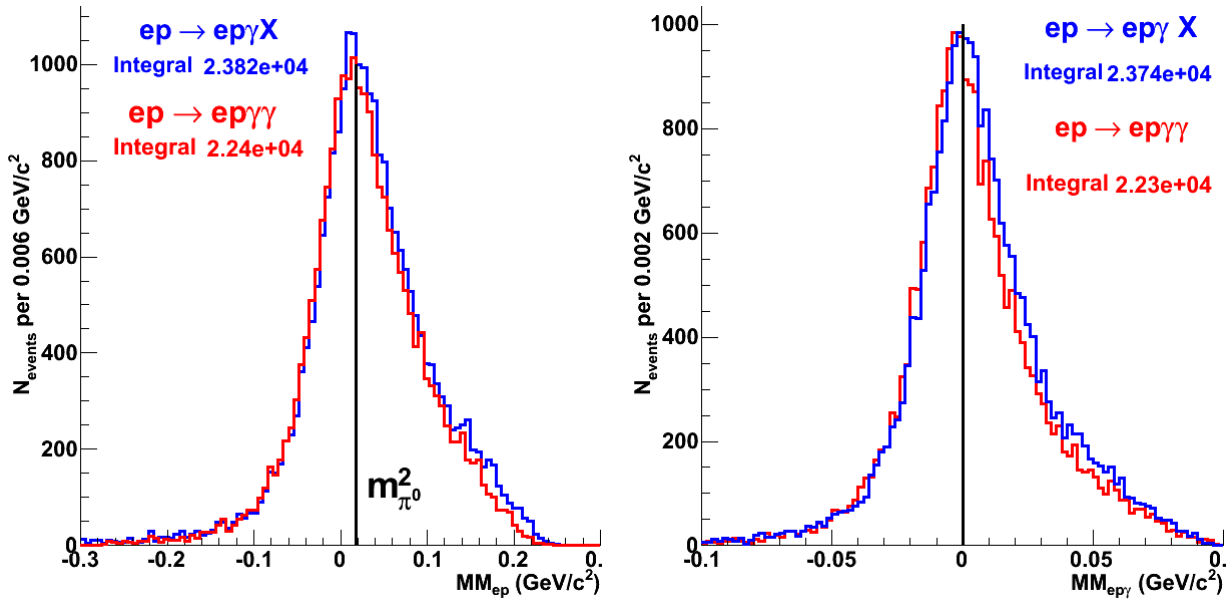

Figure 18: The red line corresponds to the data tree where both photons were detected and the line in blue corresponds to the data tree where the second photon was predicted. Comparing the integrals of the blue line and the red line gives an estimate of the EC efficiency that is close to what has been theoretically expected.

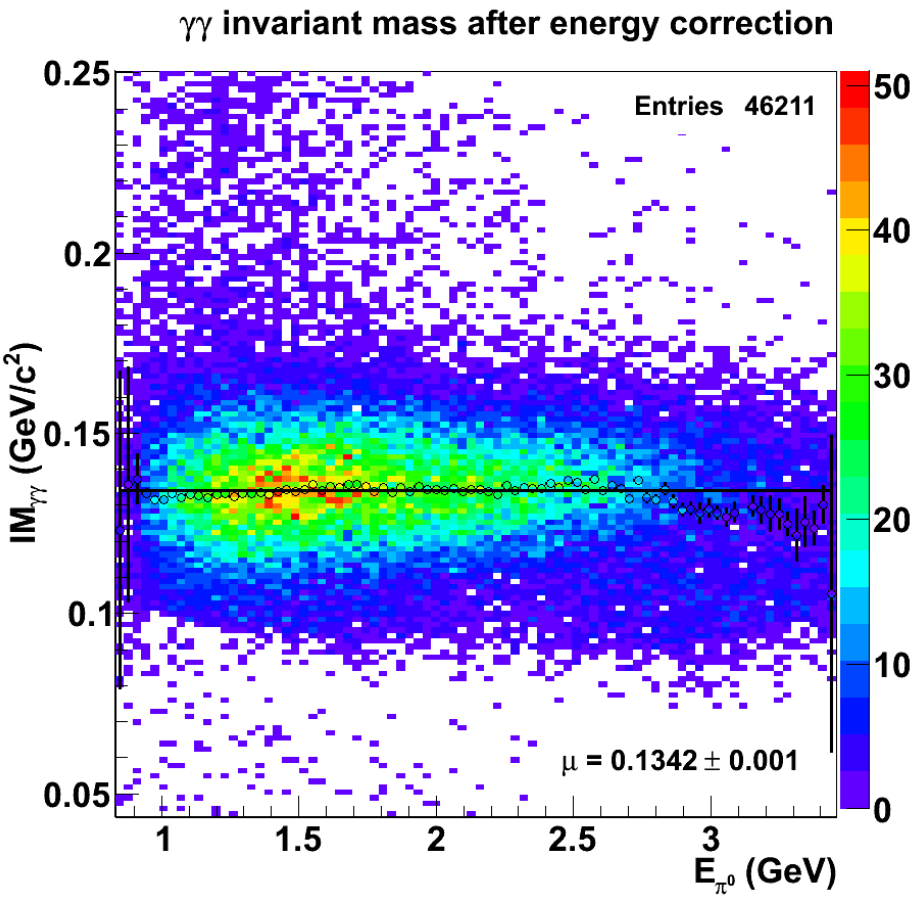

Figure 19: The invariant mass of the two photons using the energy correction function as a function of the energy of the neutral pi meson. The mean value of the invariant mass is 0.1342 GeV/c^2.

ACKNOWLEDGEMENTS

I would like to thank my mentor, Francois-Xavier Girod, for sharing his knowledge and guiding me through the process. This research was conducted at the Thomas Jefferson National Accelerator Facility (Jefferson Lab). I thank the U.S. Department of Energy, Office of Science for making it possible for me to participate in the SULI program.

REFERENCES

[1] Nuclear Physics, Thomas Jefferson National Accelerator Facility, "Generalized Parton Distributions (GPDs)," November 2008, http://www.jlab.org/highlights/phys.html#gpd.

[2] P. Schewe, B. Stein, and D. Castelvechhi, “Tomography of Protons,” January 22, 2007, http://www.aip.org/pnu/2007/split/809-2.html.

[3] B.A. Mecking et al., “The CEBAF large acceptance spectrometer (CLAS),” in *Nuclear Instruments and methods in Physics Research A,* Elsevier Science B.V., 2003, pp.513-33.

[4] F.-X. Girod, July 09, 2009.

[5] V. Burkert et al., CLAS-NOTE 2002-006, 2002, http://www1.jlab.org/ul/Physics/Hall-B/clas.

[6] R. De Masi et al., CLAS-NOTE 2006-015, 2006, http://www1.jlab.org/ul/Physics/Hall-B/clas.

[7] F.-X. Girod, July 27, 2009.

[8] Hyon-Suk Jo, "DVCS cross-sections with CLAS", *IPN-Orsay PhD thesis*. March 2007.